

# Effects of Soil Electromagnetic Properties on Metal Detectors

Yogadish Das, *Fellow, IEEE*

**Abstract**—This paper presents an analysis, based on existing work in geophysics and nondestructive testing, of the effects of soil electromagnetic properties on the functioning of metal detectors widely used to detect buried landmines. The host soil is modeled as a half-space having real and frequency-independent electrical conductivity but frequency-dependent complex magnetic susceptibility. The analysis technique has been applied to three examples of soil of practical importance, namely, nonconducting soil with frequency-independent susceptibility, nonconducting soil with frequency-dependent susceptibility, and nonmagnetic soil with constant conductivity. Simplifications are made to clearly explain a number of previous field and experimental observations, for example, the greater influence of magnetic properties than of electrical conductivity on the performance of metal detectors. Results also show that soil magnetic properties affect continuous wave and pulsed-induction detectors differently. The effect that electrical conductivity and magnetic susceptibility of the host soil have on the signal produced by a target is investigated by computing the response of a buried small metallic sphere. Computations show that in some cases, which could represent practical landmine detection scenarios, the signal from the soil can dominate that due to the target, making it hard to detect the target. Further, it is shown that magnetic soil can alter a target's spectral response, which implies that, contrary to present practice, object identification techniques should take into account the electromagnetic parameters of the host medium.

**Index Terms**—Humanitarian demining, landmine detection, soil electrical conductivity, soil electromagnetic properties, soil magnetic susceptibility, world soil database.

## I. INTRODUCTION

THE metal detector is one of the most commonly used detection tools in humanitarian demining. The adverse effect of certain types of soil on metal detectors was recognized during World War II [1], [2]. During the period 1945–1947, the effect of different rocks and soils on the performance of the U.S. SCR-625 mine detector was studied [3]. A summary of some aspects of U.S. research from this era on the implication of magnetic soil for mine detection can be found in [4]. In the intervening time since these studies were done, the issue of dependence of metal detector performance on soil properties appears to have kept a low profile in the mine detection community. Any subsequent research that was done on this topic appears to have been carried out by detector manufacturers, only some of whom (e.g., [5]) have publicly divulged their findings. As well, results of related earlier work [3] are also not widely

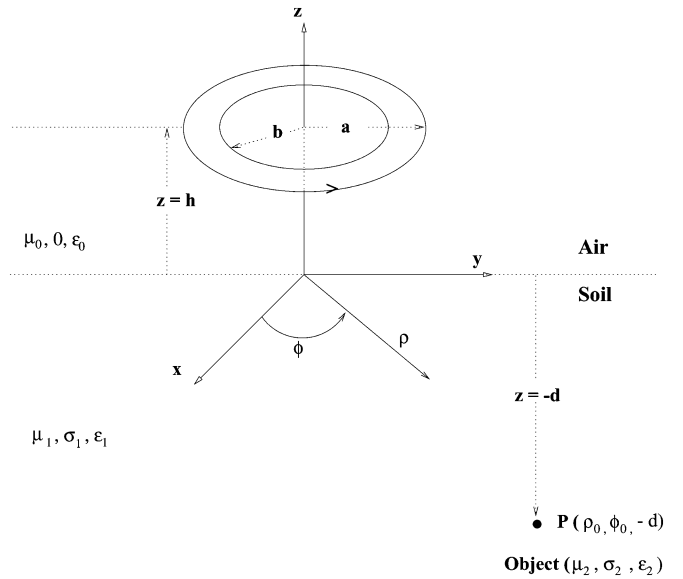


Fig. 1. Geometry of the problem.

available. Only very recently have other researchers, in mine detection and related fields, started to consider the effect of soil [6]–[10]. The cases studied in [7], [8] belong to UXO detection, investigation carried out in [6], [9] is solely experimental, and [10] treats primarily the case of frequency-independent magnetic permeability.

The operation of the metal detector is based on the principle of electromagnetic induction. The signal produced in a detector by a metal object depends on many factors including the object's size, shape, orientation, material, and the parameters of the detector electronics. One of the other important factors that can influence this signal is the host soil. A systematic analytical framework, based on well-established techniques in geophysics and nondestructive testing, for studying the effects of soil electromagnetic properties was presented in an earlier paper [11], including a discussion of the relevance and requirements of soil-related research in humanitarian demining. Results of further study and additional numerical results were included in a subsequent paper [12]. The main purpose of this paper is to consolidate and extend the work reported in these previous papers.

The analytical framework used for the computation is summarized in Section II and numerical results and observations are presented in Section III. A summary and overall conclusions are given in Section IV.

## II. ANALYSIS

The geometry employed to analyze the metal detector problem is shown in Fig. 1. For this study the soil is modeled

Manuscript received October 24, 2005; revised December 29, 2005. This work was supported by the Canadian Centre for Mine Action Technologies.

The author is with the Threat Detection Group, Defence R&D Canada—Suffield, Medicine Hat, AB, T1A 8K6 Canada (e-mail: yogadas@drdc-rddc.gc.ca).

Digital Object Identifier 10.1109/TGRS.2006.870401

as a homogeneous half-space. In keeping with a commonly found design, the metal detector head is taken to consist of a pair of concentric and coplanar circular coils. The transmitter coil radius and number of turns are respectively  $a$  and  $N_t$  while those of the receiver coil are  $b$  and  $N_r$ . The coordinate systems used, the magnetic permeability ( $\mu_j$ ), electrical conductivity ( $\sigma_j$ ) and permittivity  $\epsilon_j$  of the various regions are shown on the figure, where the subscript  $j = 0, 1, 2$  indicates air, soil, and target material, respectively. The coil assembly is at a height  $z = h$  from the air-soil interface. The transmitter current is assumed to be  $Ie^{i\omega t}$  with  $\omega = 2\pi f$ , where  $f$  is the frequency of operation. The solution to this classic half-space problem, which has been extensively investigated by many, was discussed in detail in [11] in the context of the metal detector. Expressions for electromagnetic fields in the various regions as well as for voltages induced in the receiver coil under various circumstances were given in that paper. Here, only a few selected results which are of direct relevance to the discussion of this paper will be used.

The literature on electromagnetic properties of soil is extensive and it is beyond the scope of this paper (see for example [13]–[21]). It will suffice for our purpose here to simply state the models used for the electromagnetic properties of soil in the analysis. The permittivity of soil will be assumed to be frequency-independent, the same as that of free space and will not be considered in the results (i.e., displacement currents will be ignored). Electrical conductivity ( $\sigma_1$ ) will also be assumed to be frequency-independent. Magnetic behavior is assumed to be frequency-dependent in the general case and is modeled as follows:

$$\mu_1 = \mu_0(1 + \chi(\omega)) \quad (1)$$

$$\begin{aligned} \chi(\omega) &= \chi'(\omega) + i\chi''(\omega) \\ &= \chi_0 \left( 1 - \frac{1}{\ln(\tau_2/\tau_1)} \cdot \ln \frac{i\omega\tau_2 + 1}{i\omega\tau_1 + 1} \right) \end{aligned} \quad (2)$$

where  $\mu_0$  and  $\mu_1$  are the magnetic permeability of free-space and soil respectively.  $\chi(\omega)$  is the complex frequency-dependent susceptibility of soil with real and imaginary components  $\chi'$  and  $\chi''$  respectively, while  $\chi_0$  is the d.c. value of susceptibility. The particular model of susceptibility represented by (2) arises from assuming that the distribution of magnetic relaxation time constants is log-uniform; explicitly,  $\ln \tau$  is distributed uniformly between  $\ln \tau_1$  and  $\ln \tau_2$ . This model, which is discussed in Chikazumi [22] and elsewhere [17], [23], is believed to be due to Richter [24]. This model is widely used to represent soils that display magnetic viscosity. Such soils are common in many landmine-affected regions of the world.

Extensive measured data on susceptibility spectrums of a range of real soils are not currently available, which makes the choice of model parameters difficult. Although the limited data that are available [20], [25] may indicate a wider range of relaxation time constants in most cases, for the numerical computations presented in this paper, values for  $\tau_1$  and  $\tau_2$  are chosen, albeit somewhat arbitrarily, to be  $10^{-6}$  s and  $10^{-3}$  s, respectively. The particular susceptibility model resulting from this choice of parameters is shown in Fig. 2, which shows the variation of the real and imaginary parts of  $\chi/\chi_0$  over the frequency band of interest for metal detectors. The particular

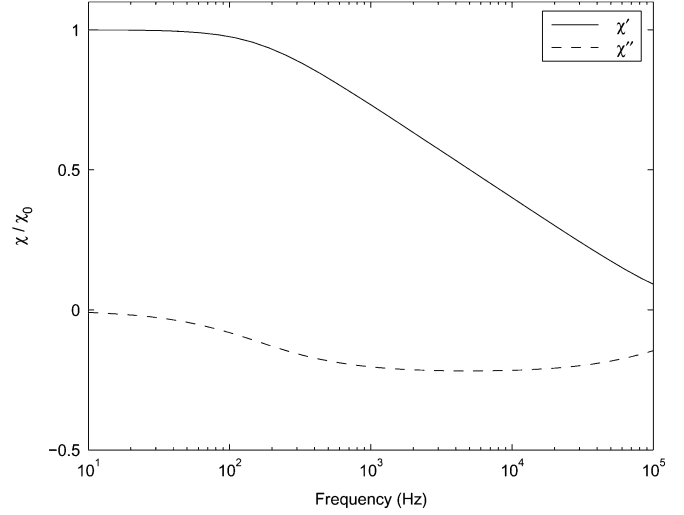


Fig. 2. Model for frequency-dependent soil susceptibility used in this paper. The real and imaginary parts of  $\chi$  are computed using (2) with  $\tau_1 = 10^{-6}$  s and  $\tau_2 = 10^{-3}$  s.

choice of parameters preserves the general character of the model, namely, the nonlinear variation of susceptibility with logarithm of frequency. Of course, the calculations can be carried out just as easily using other values of  $\tau_1$  and  $\tau_2$ , as required, for a given soil. For our primary purpose here, which is to demonstrate the phenomenon of the influence of soil susceptibility on target response, it is not essential to use actual values of these parameters for real-world soils. Experimental validation of soil models and the sensitivity of detector response to variation in model parameters will be studied in the future.

Analysis of induction systems is commonly carried out in terms of the magnetic fields involved and their time derivative. However, in this analysis the voltage induced in the receiver coil will be used since it is the directly measured quantity in a metal detector. Using the results from [11], [12] one can write down the expressions for induced voltages under various conditions.

In the absence of soil or target, the induced voltage normalized by the product  $N_t N_r I$ , can be written as

$$v^{\text{air}} = i\mu_0 \omega \pi ab \int_0^\infty J_1(\lambda a) J_1(\lambda b) d\lambda \quad (3)$$

where  $J_1$  denotes a Bessel function of the first kind and order 1 and  $\lambda$  is an integration variable.

Similarly, the normalized induced voltage,  $v^{\text{soil}}$ , due only to the presence of the soil is given by

$$\begin{aligned} v^{\text{soil}} &= i\mu_0 \omega \pi ab \int_0^\infty \Gamma(\lambda, u_1, \chi) \\ &\quad \times J_1(\lambda a) J_1(\lambda b) \exp(-2\lambda h) d\lambda \end{aligned} \quad (4)$$

with

$$\Gamma(\lambda, u_1, \chi) = \frac{\lambda(1 + \chi) - u_1}{\lambda(1 + \chi) + u_1}$$

where  $u_1 = \sqrt{\lambda^2 + i\sigma_1 \mu_0 \omega}$ .

#### A. Induced Voltage When a Buried Target Is Present

A well-known approximation technique [26], [27] was used to obtain an expression for the voltage induced in a receiver coil

by a buried target. In this approach, the buried object is replaced with an equivalent magnetic dipole,  $\vec{M}$ , and a current dipole,  $\vec{P}$ , and the principle of reciprocity is used to obtain the induced voltage. As shown in [11], the voltage  $V^{\text{target}}$  induced in the receiver coil by a buried spherical target can be written as

$$V^{\text{target}} = i\omega\mu_0 (H_{1\rho}^b M_\rho + H_{1z}^b M_z) + E_{1\phi}^b P_\phi \quad (5)$$

where  $H_{1\rho}^b$ ,  $H_{1z}^b$ , and  $E_{1\phi}^b$  are the indicated components of magnetic and electric field intensities that would be produced in soil at the location of the equivalent dipole (sphere centre in this case) if a unit current were flowing in the receiver coil of radius,  $b$ .  $M_\rho$ ,  $M_z$ , and  $P_\phi$  are the components of the scatterer equivalent dipole moments  $\vec{M}$  and  $\vec{P}$  which depend on the inducing fields  $H_{1\rho}$ ,  $H_{1z}$ , and  $E_{1\phi}$  produced at the sphere centre by the transmitter current. For a sphere of radius,  $R$ , and electrical parameters,  $(\mu_2, \epsilon_2, \sigma_2)$ , embedded in a half-space with parameters  $(\mu_1, \epsilon_1, \sigma_1)$ , the components of the dipole moments can be obtained from

$$\vec{M} = -2\pi R^3 (H_{1\rho} \hat{a}_\rho + H_{1z} \hat{a}_z) \frac{N_1}{D_1} \quad (6)$$

where  $N_1$  and  $D_1$  are given by

$$N_1 = [\mu_1 (1 + k_2^2 R^2) + 2\mu_2] \sinh(k_2 R) - (2\mu_2 + \mu_1) k_2 R \cosh(k_2 R) \quad (7)$$

$$D_1 = [\mu_1 (1 + k_2^2 R^2) - \mu_2] \sinh(k_2 R) + (\mu_2 - \mu_1) k_2 R \cosh(k_2 R) \quad (8)$$

$$\vec{P} = -2\pi R^3 \sigma_1 E_{1\phi} \hat{a}_\phi \frac{N_2}{D_2} \quad (9)$$

where  $N_2$  and  $D_2$  are given by

$$N_2 = [\sigma_1 (1 + k_2^2 R^2) + 2\sigma_2] \sinh(k_2 R) - (2\sigma_2 + \sigma_1) k_2 R \cosh(k_2 R) \quad (10)$$

$$D_2 = [\sigma_1 (1 + k_2^2 R^2) - \sigma_2] \sinh(k_2 R) + (\sigma_2 - \sigma_1) k_2 R \cosh(k_2 R) \quad (11)$$

where  $(\hat{a}_\rho, \hat{a}_\phi, \hat{a}_z)$  are the cylindrical coordinate unit vectors and  $k_2^2 = i\sigma_2\mu_2\omega$ . A study of the conditions under which the above approximations, represented by (5)–(11), are reasonable is outside the scope of this paper. For a general discussion of the assumptions used in deriving these equations one could consult [26]–[29]. However, the accuracy achieved in practice can be established only by comparing the approximate results with those obtained from experiments, rigorous analysis or numerical computations for cases typical of the application concerned.

Explicit expressions derived in [11] for the fields in soil, namely,  $H_{1\rho}$ ,  $H_{1z}$ , and  $E_{1\phi}$  are included in the Appendix for ready reference. The fields  $H_{1\rho}^b$ ,  $H_{1z}^b$ , and  $E_{1\phi}^b$  can be obtained from (28)–(30) by simply replacing  $a$  with  $b$  and setting  $I = 1$ . The values of the dipole moment components from (6) and (9) can be used in (5) to calculate the voltage induced by a buried spherical target. Obviously, the number of turns in each coil must be taken into account if the absolute value of the induced voltage is desired. Although both the magnetic and the current dipole have been included, considering only the magnetic

dipole contribution is often sufficient, particularly when the soil conductivity,  $\sigma_1$ , is very low which is often the case. As well, for an on-axis target there is no contribution from the current dipole since  $E_{1\phi} = 0$  on axis. Numerical results presented in this paper will consider only the magnetic dipole moment.

### III. RESULTS AND DISCUSSION

The effect that soil electromagnetic properties have on the performance of a metal detector has a number of aspects: (a) There is a signal produced by the soil itself as given by (4). This is the “background” signal against which buried targets need to be detected. In some cases this signal could be much larger than that produced by the target being sought, making the target difficult to detect. If in addition, as is the case in practice, the soil properties vary spatially, the signal produced by the soil could appear to be that produced by a target, thus generating false alarms. (b) The intensity of the inducing electromagnetic fields  $H_{1\rho}$ ,  $H_{1z}$ , and  $E_{1\phi}$  will be different in the soil than their values in free space. As seen from (6) and (9) this, in part, will affect the values of the induced target moments which contribute to the signal  $V^{\text{target}}$  generated by the target (5). Similarly, soil will have an effect on the intensity of the receiver fields  $H_{1\rho}^b$ ,  $H_{1z}^b$ , and  $E_{1\phi}^b$  which will also influence the target signal. (c) A subtle and interesting effect of soil is through the complex “response function”  $(N_1)/(D_1) \equiv X + iY$  in (6), which describes the scattering properties of the object in a host medium and is commonly used in the literature [30] to characterize the operation of electromagnetic induction systems. Functions  $X$  and  $Y$  are usually assumed to depend only on target properties and as a result are used to identify targets (see for example [31]). However, host soil can change these fundamental target features as expected from (7) and (8) and discussed in Section III-C.

Available space does not allow analysis and presentation of data on all aspects of the effect of soil. Limited results for only three types of soil and one target will be included to illustrate the basic nature of soil metal detector interaction and provide a simple explanation for previous experimental observations.

Characteristics of the signal due to soil alone and their effect on frequency and time-domain detectors are discussed in Sections III-A and III-B. In that discussion, reference is made to an *ad hoc* method used by deminers in the field to empirically characterize soil, which, for lack of a standard or better term, is called the “reference height method” (RHM). In this method [3], [9], [32], which seems to have been independently discovered some 50 years apart, the effect of the soil is quantified by measuring the distance of the sensor head to the ground surface at which a chosen metal detector, that does not incorporate soil compensation, produces a preselected level of response. Suitability of this method under various circumstances is discussed.

Effects of soil on target signal are discussed in Section III-C. Results are restricted to the frequency domain and only the case of a nonpermeable conducting small sphere located on the axis of a detector system is considered. The frequency range of investigation is restricted to 0–100 kHz which covers the bandwidth used by present metal detectors. The transmitter and receiver coil radii of 0.12 and 0.09025 m, respectively, which are the values used in a familiar detector (Schiebel AN19/2), are used

in the computations. The target used is restricted to a small aluminum sphere with radius  $R=0.005$  m,  $\sigma_2=3.54\times10^7$  S/m and, as already stated, only the case of an on-axis target is presented. Only three types of soil will be considered—nonconducting soil with frequency-independent susceptibility, nonconducting soil with frequency-dependent susceptibility and nonmagnetic soil with constant conductivity.

#### A. Soil Signal: Nonconducting Magnetic Soil

If the soil is nonconducting ( $\sigma_1=0$ ) but magnetic with a susceptibility  $\chi(\omega)$ , then from (4) the normalized voltage induced in the receiver coil due to the soil alone can be written as

$$v^{\text{soil}} = i\mu_0\omega\pi ab \left[ \frac{\chi(\omega)}{2+\chi(\omega)} \right] m(h) \quad (12)$$

which reduces to the following for soils with frequency-independent real susceptibility (i.e.,  $\chi(\omega)=\chi_0$ ):

$$v^{\text{soil}} = i\mu_0\omega\pi ab \left[ \frac{\chi_0}{2+\chi_0} \right] m(h) \quad (13)$$

where  $m(h) = \int_0^\infty J_1(\lambda a)J_1(\lambda b) \exp(-2\lambda h) d\lambda$ .

Using integral no. 17 in [33, p. 316] one can write  $m(h)$  as follows:

$$m(h) = \frac{2}{\pi k\sqrt{ab}} \left[ \left( 1 - \frac{1}{2}k^2 \right) K - E \right] \quad (14)$$

where  $k^2 = (4ab)/((a+b)^2 + 4h^2)$  and  $K$  and  $E$  are complete elliptic integrals of the first and second kind respectively, defined as  $K = \int_0^{\pi/2} (1-k^2 \sin^2 \theta)^{-1/2} d\theta$  and  $E = \int_0^{\pi/2} (1-k^2 \sin^2 \theta)^{1/2} d\theta$ .

A lot can be learned about the nature of the signal produced by soil and its implication for metal detectors from an examination of (12) and (13). The various aspects of soil response have been discussed in detail in [11]. Here, only a brief summary of the main findings will be given.

Equation (12) can be used to model real-world “lateritic” soil in some cases, where the conductivity is very low because of the particular clay type involved and the particle size distribution of the magnetic constituents in the soil gives rise to magnetic viscosity. This type of soil is quite common in mine-affected tropical regions. On the other hand, (13) can be used to model soil that does not show susceptibility dispersion (for example, soil containing only coarse grain magnetite). These two types of soil respond very differently to the operation of metal detectors as highlighted below.

##### 1) Soil With Frequency-Independent Susceptibility:

- The background signal produced in a frequency-domain detector by soil with frequency-independent susceptibility is purely imaginary and is linearly dependent on frequency.
- Since  $m(h)$  is a function only of the sensor height  $h$  above ground, the output voltage at a given frequency can be calibrated in terms of soil susceptibility ( $\chi_0$ ) if the measurement height is known. In other words, if the RHM is used with a frequency-domain detector over such a soil, the value of  $m(h)$  at the reference height can be related to soil susceptibility and the reference height will give an indication of the “badness” of the soil for such detectors.

- In the time-domain, a step-current excitation results in the following response:

$$v_{\text{step}}^{\text{soil}}(t) = \left[ \mu_0\pi ab \frac{\chi_0}{2+\chi_0} m(h) \right] \delta(t) \quad (15)$$

where  $\delta(t)$  is the Dirac delta function. The above relation implies that the response to a step excitation is concentrated only at the time where the step changes state ( $t=0$ ). Hence for measurements taken at times,  $t > 0$ , which is the case in pulsed-induction detectors there would be no contribution from the soil. Thus, in theory at least, such soils would not affect the performance of pulsed induction detectors. If such a detector is used in the RHM mode it would give a zero reference height for all such soils irrespective of their magnetic susceptibility and as a result would be unsuitable to indicate how well a frequency-domain detector might work over such soils.

##### 2) Soil With Frequency-Dependent Susceptibility:

- In contrast to soil with frequency-independent susceptibility, the response of soil with frequency-dependent susceptibility will have both a real and an imaginary component, which can be shown to be

$$v_{\text{real}}^{\text{soil}} = \mu_0\pi ab\omega \left[ \frac{-2\chi''(\omega)}{[\chi'(\omega)+2]^2 + \chi''(\omega)^2} \right] m(h) \quad (16)$$

$$v_{\text{imag}}^{\text{soil}} = \mu_0\pi ab\omega \left[ \frac{\chi'(\omega)^2 + 2\chi'(\omega) + \chi''(\omega)^2}{[\chi'(\omega)+2]^2 + \chi''(\omega)^2} \right] m(h). \quad (17)$$

These relations imply that if a frequency-domain system measures both the real and imaginary components of the induced voltage separately at a known frequency then the  $\chi'$  and  $\chi''$  at the measurement frequency can be estimated, in principle, by solving two simultaneous quadratic equations. If only the amplitude of the voltage is measured, as is often the case in metal detectors, then  $\chi'$  and  $\chi''$  cannot be separately estimated without further assumptions on their relationships. The reference height measured using the RHM will be a rather complicated function of both  $\chi'$  and  $\chi''$ .

- If a soil is only very weakly magnetic ( $|\chi| \ll 1$ , which is commonly the case with natural soils), one can approximate the term in brackets in (12) by  $(\chi(\omega))/(2)$  and as shown in [11] can derive an approximate but simple expression for the step response for  $t > 0$

$$v_{\text{step}}^{\text{soil}}(t) \approx \mu_0\pi abm(h) \frac{\chi_0}{2\ln(\tau_2/\tau_1)} \cdot \frac{1}{t} \quad (18)$$

where measurement times and parameter values are such that  $(t)/(\tau_1) \gg 1$  and  $(t)/(\tau_2) \ll 1$ . The transient response of magnetically viscous host media has been treated much more rigorously by Lee [23], [34] for coincident-loop systems in geophysics. However, it seems that the simple time variation ( $1/t$ ) expressed by (18), which is in agreement with the early experimental observation reported in [35], is all that is often used in practice. As an example, Candy [5] uses the following functional form for

the decay of the induced voltage due to a ramp current excitation of duration  $T$  in the design of a metal detector that compensates very well for interference from most magnetic soils

$$v(t) \propto \ln \frac{T+t}{t} - \frac{T}{t} \quad (19)$$

where  $t$  is measured from the turn-off of the ramp. This relationship can be derived by assuming a  $(1/t)$  step response and applying Laplace transform theory to compute the response to a finite ramp.<sup>1</sup>

- From (15), (18), and (19), it is clear that unlike in the case of frequency-independent soil, the transient signal due to magnetically viscous soil will persist long after the turning off of the transmitter current pulse and may be confused as signal produced by a buried metal object.
- If a time-domain system is used for RHM over such a soil, then the reference height measured for a single time window (say,  $t = t_1$ ), which is commonly the case, will give an indication of the factor  $(\chi_0)/(2 \ln(\tau_2/\tau_1))$ . If measurements of  $v_{\text{step}}^{\text{soil}}(t)$  are available over a time range one could in principle estimate the values of  $\tau_1$  and  $\tau_2$  by nonlinear fitting.
- Under certain conditions, namely,  $\omega\tau_1 \ll 1$  and  $\omega\tau_2 \gg 1$ , it can be shown from (2) that

$$\frac{\partial \chi'}{\partial \ln \omega} = \frac{2}{\pi} \chi'' = -\frac{\chi_0}{\ln(\tau_2/\tau_1)}. \quad (20)$$

According to this relationship which has been discussed in detail by others [7], [18], [20] the slope of the real part of susceptibility is constant and is proportional to its imaginary part. When (20) holds, one can write from (18)

$$\begin{aligned} v_{\text{step}}^{\text{soil}}(t) &= -\mu_0 \pi abm(h) \frac{\chi''}{\pi} \cdot \frac{1}{t} \\ &= -\frac{1}{2} \mu_0 \pi abm(h) \cdot \frac{\partial \chi'}{\partial \ln \omega} \cdot \frac{1}{t}. \end{aligned} \quad (21)$$

The above imply that the induced voltage measured at a given time is proportional to the imaginary part of susceptibility or equivalently to the slope of its real part. Hence, RHM using a time-domain system over such soils would give a reference height which is indicative of this slope or equivalently of magnetic loss. This result, in part, explains the experimental observation reported in [9]<sup>2</sup> where reference heights were seen to correlate with the difference in susceptibility at two frequencies. That paper also indicates a correlation between reference heights and “average signal” measured by a time-domain instrument (see [9, Fig. 5]). This equivalent time-domain observation can also be explained from (21).

### B. Soil Signal: Conducting Nonmagnetic Soil

The case of conducting but nonmagnetic ground has been extensively treated in geophysics (see, for example, [36] for a review). Here, a few well-known results will simply be applied to the case of the metal detector. These results, with some rough approximations, will then be used to obtain an expression for the

<sup>1</sup>An alternate derivation is discussed in [8].

<sup>2</sup>Communication with the authors confirmed that data for lane 5 in [9, Fig. 4] are invalid due to an unnoticed measurement error.

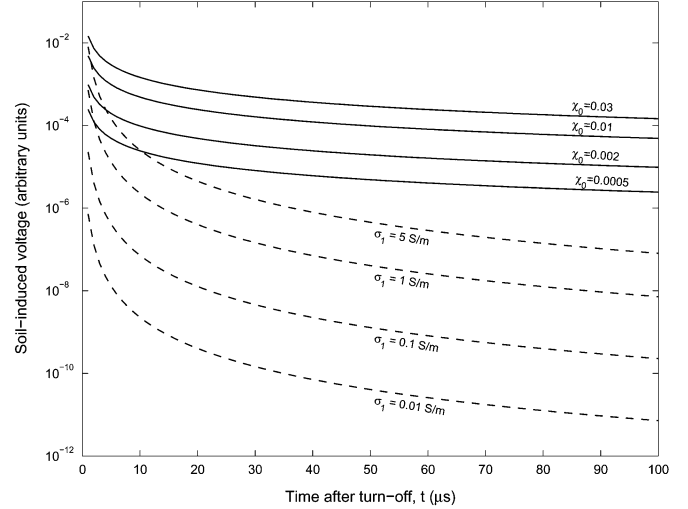


Fig. 3. Relative contributions of conductivity and frequency-dependent susceptibility to the signal produced by soil in a metal detector. Values of magnetic relaxation time constants used are  $\tau_1 = 10^{-6}$  s and  $\tau_2 = 10^{-3}$  s.

induced voltage which will allow one to make preliminary conclusions on the relative influence of soil conductivity and soil susceptibility. From (4), the induced voltage can be written as (putting  $\chi = 0$ )

$$\begin{aligned} v^{\text{soil}} &= i\mu_0 \omega \pi ab \int_0^\infty \frac{\lambda - \sqrt{\lambda^2 + i\sigma_1 \mu_0 \omega}}{\lambda + \sqrt{\lambda^2 + i\sigma_1 \mu_0 \omega}} \\ &\quad \times J_1(\lambda a) J_1(\lambda b) \exp(-2\lambda h) d\lambda. \end{aligned} \quad (22)$$

An analytical solution for the general case where  $h \neq 0$  and  $a \neq b$  does not appear to be available and that case is best handled numerically both in time and frequency domains. However, the case of coincident loops ( $a = b$ ) lying on the ground ( $h = 0$ ) has been treated by many. For example, by applying the procedure discussed in [37] to (22), one can write down the following expression (for  $t > 0$ ) for the normalized voltage induced due to a step current that turns off at  $t = 0$ :

$$v_{\text{step}}^{\text{soil}}(t) = \frac{\mu_0 \sqrt{\pi} a}{t} \cdot F(t) \quad (23)$$

where  $F(t)$  is given by

$$\begin{aligned} F(t) &= \sqrt{\frac{\sigma_1 \mu_0 a^2}{t}} \sum_{m=0}^{\infty} \frac{(-1)^m}{m!} \frac{(2m+2)!}{(m+1)!(m+2)!(2m+5)} \\ &\quad \times \left( \frac{\sigma_1 \mu_0 a^2}{4t} \right)^{m+1}. \end{aligned} \quad (24)$$

Keeping only the  $m = 0$  term leads to the following often-quoted “late-time” approximation [8], [36] in geophysics

$$v_{\text{step}}^{\text{soil}}(t) \approx \pi a^2 \frac{\sigma_1^{3/2} \mu_0^{5/2} a^2}{20\sqrt{\pi}} t^{-5/2}. \quad (25)$$

It is clear from (18) and (25) that the signal due to conductivity decays much faster with time than that due to soil magnetic viscosity. Nevertheless, a simple example is included to illustrate this, which should give an indication of the relative importance of these two soil parameters in the performance of metal detectors. Fig. 3 shows the induced voltage as a function of time after turn-off of a step current excitation for a number of conducting but nonmagnetic and nonconducting but magnetically lossy half-spaces. Conductivities used range from 0.01 S/m, a

typical value for soils, to a high value of 5 S/m which is likely higher than the conductivity of sea water-saturated soil. Susceptibility values range from 0.0005 SI units, representing a weakly magnetic soil, to 0.03 SI units, which, although not the highest value found in natural soils, is typical of some soils known to have severely limited the performance of metal detectors. Values of magnetic relaxation time constants were assumed to be  $\tau_1 = 10^{-6}$  s and  $\tau_2 = 10^{-3}$  s. The transmitter and receiver coil radii of 0.12 and 0.09025 m, respectively, which are the sizes used in a very common (Schiebel AN19/2) mine detector, were used in the calculations for the magnetic soil. In order to use the available simple equation for the conductive half-space, only coincident loops ( $a = 0.12$  m) were considered, which would result in a slightly higher estimate for the induced voltage than if a receiver coil of smaller diameter was used. Note that loops were assumed to lay on the ground ( $h = 0$ ) for these simulations.

An examination of Fig. 3 clearly shows that the influence of soil magnetic properties far exceeds that of soil conductivity on the performance of metal detectors.<sup>3</sup> Even comparing the extreme cases of the most conducting ( $\sigma_1 = 5$  S/m) soil and the least magnetic ( $\chi_0 = 0.0005$  SI units) soil, one can see that the magnetic contribution exceeds the conductivity contribution after about 13  $\mu$ s, a time much lower than the first measurement window in a typical detector. For the other cases shown, the magnetic contribution exceeds, by orders of magnitude in some cases, the contribution due to soil conductivity. Also in these cases, the magnetic contribution exceeds that due to conductivity at measurement times much shorter than 13  $\mu$ s. These observations partially corroborate previous experimental findings [6].

### C. Target Signal: Nonconducting Magnetic Soil

The voltage induced in the receiver coil is the quantity measured in practice and contributions to this voltage from the soil and the target will be computed to assess the overall effect of soil on detector performance. However, important insight into the effect of soil on the signal produced by the target is obtained by studying the response functions  $X$  and  $Y$  themselves. In that regard, the following limiting expressions for the response functions will be helpful. It can be shown<sup>4</sup> from (7) and (8) that for  $|k_2 R| \rightarrow 0$

$$\begin{aligned} X + iY &= -2 \left( \frac{\mu_2 - \mu_1}{\mu_2 + 2\mu_1} \right) \\ &\quad + i \frac{\sigma_2 \mu_1 \omega R^2}{15} \left( \frac{3\mu_2}{\mu_2 + 2\mu_1} \right)^2 + \dots \\ &= \frac{2\chi}{2\chi + 3} + i \frac{9}{15} \sigma_2 \mu_0 \omega R^2 \frac{1 + \chi}{(2\chi + 3)^2} + \dots \quad (26) \end{aligned}$$

when the sphere material is nonmagnetic (i.e.,  $\mu_2 = \mu_0$ ) and  $\mu_1$  is replaced with  $\mu_1 = \mu_0(1 + \chi)$ .

Similarly, for  $|k_2 R| \rightarrow \infty$

$$X + iY = 1. \quad (27)$$

<sup>3</sup>Strictly speaking, data presented here support this conclusion only for time-domain systems in one geometry. Analysis of frequency-domain systems and other geometries will be undertaken in the future.

<sup>4</sup>Similar results appearing in the very well-known text by Grant and West [30, Eqs. (17)–(15)] have errors in them.

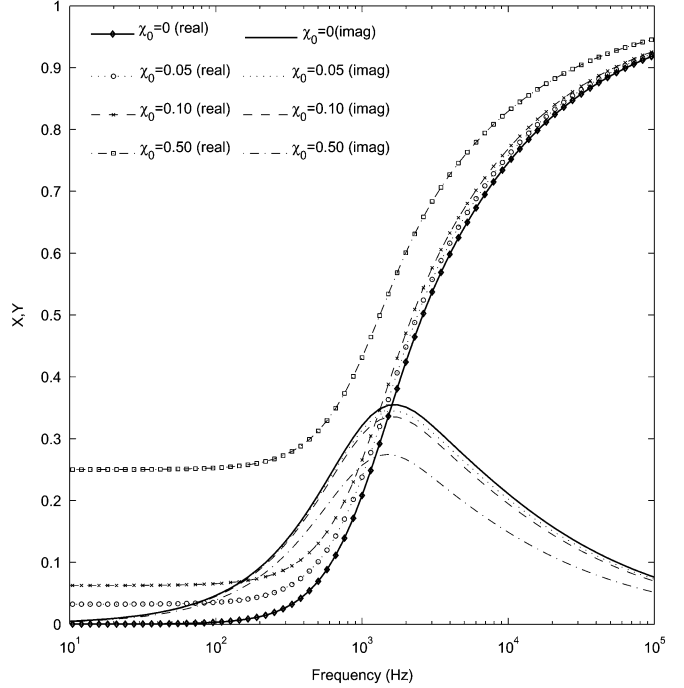


Fig. 4. Effect of frequency-independent soil on the response functions of an aluminum sphere of radius  $R = 0.005$  m, conductivity  $\sigma_2 = 3.54 \times 10^7$  S/m.

1) *Soil With Frequency-Independent Susceptibility*: Fig. 4 shows the response functions for the aluminum sphere embedded in soil of various susceptibility values in the range 0–0.5 which should cover most naturally occurring soil of this type. An examination of the figure shows the following.

- The response function of a sphere buried in magnetic soil is different from that when it is in free space ( $\chi_0 = 0$ ). A susceptibility value as low as 0.05 is seen to have a noticeable effect particularly on  $X$  at lower frequencies, a behavior clearly explained by (26).
- In general, the real part of the response function increases with increasing soil susceptibility while the corresponding imaginary part decreases over the frequency band of interest. At the upper frequency limit, the response function tends to its free-space behavior as expected from (27).
- For a sphere in free space there is only one frequency at which the real and the imaginary parts intersect. This unique cross-over frequency is often proposed as a target identifier. As the graphs show there can be more than one such cross-over point (see, for example, the case of  $\chi_0 = 0.05$ ) in some cases, while in others the two parts do not intersect at all, over the frequency band of interest. This implies that target identification methods based on free-space response functions may not work when the targets are buried in magnetic soil.

In Fig. 5, the voltage induced by the soil in the absence of a target is compared with that produced by the buried target alone for two representative values of susceptibility, namely,  $\chi_0 = 0.05$  and 0.5. In practice, the observed voltage would be the sum of these two voltages and the detector would have to discern the presence of a target from this combined signal. The signal due to the soil was computed using (13) and (14), while the target

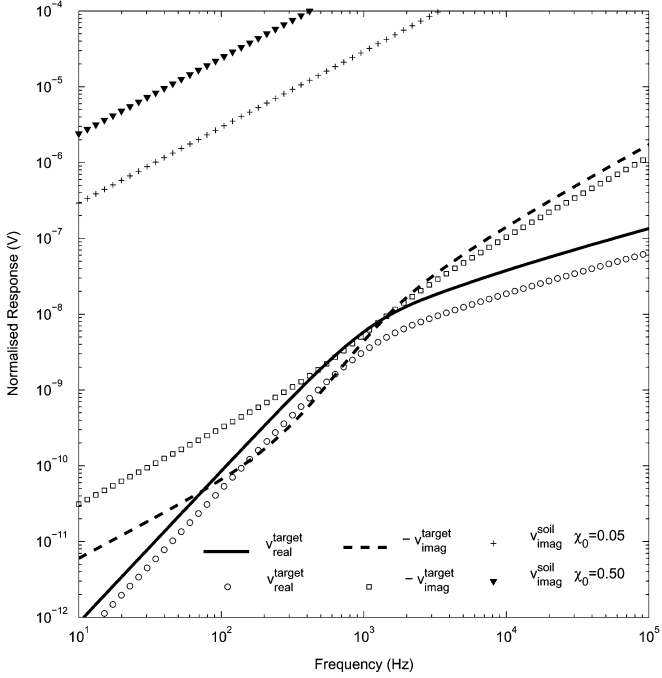


Fig. 5. Complex response of a spherical target buried in nonconducting soil with frequency-independent susceptibility. Response of the soil alone is also plotted for comparison. Sensor standoff  $h = 0$  m, object depth  $d = 0.1$  m, soil conductivity  $\sigma_1 = 0$  S/m.

response was computed using (5) and (6). An implementation<sup>5</sup> in Matlab of a well-known algorithm widely used in geophysics [38] was used to compute the required magnetic field intensities from (29). The following observations are made from the figure.

- The response due to the soil alone, which is purely imaginary, dominates the signal due to the buried target being considered, even for a soil of susceptibility  $\chi_0 = 0.05$ . As a result, a detector that measures only the signal amplitude may have difficulty to detect the presence of the target in this case. A detector designed to measure both the real and imaginary parts of the signal and suitably process them will, in principle, be able to detect the target.
- Observations about the points of intersection made on the response function of the sphere from Fig. 4 also apply to the target signal shown in Fig. 5.

2) *Soil With Frequency-Dependent Susceptibility*: As discussed earlier, unlike the case of frequency-independent soil, the response of this type of soil has both a real and an imaginary component.

Fig. 6 compares the response functions of the aluminum sphere embedded in frequency-independent soil and in soil with frequency-dependent susceptibility. A high value (0.5) for the static (d.c.) susceptibility,  $\chi_0$ , is purposely chosen to emphasize the effect of soil. The following observations are made from the figure.

- The response functions of the sphere in frequency-independent soil are different from those produced when it is buried in soil with frequency-dependent susceptibility.

<sup>5</sup>See <http://www.nmt.edu/~borchers/>. Hankel transform routines in MATLAB. hankel.html. This is a Matlab implementation of the algorithm for numerical approximation of Hankel transforms of order 0 and 1 described in [38]. The routines are available online (accessed December 22, 2004)

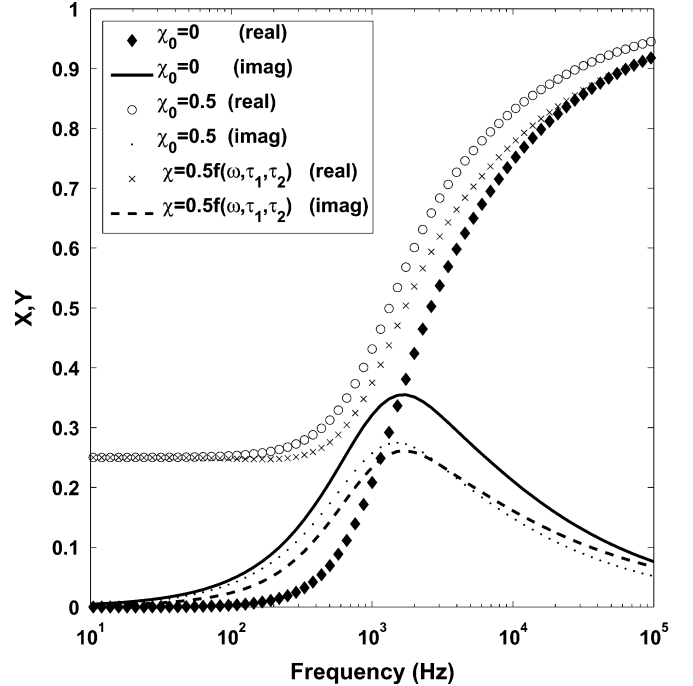


Fig. 6. Effect of soil with frequency-dependent susceptibility compared with that of frequency-independent soil on the response functions of an aluminum sphere of radius  $R = 0.005$  m, conductivity  $\sigma_2 = 3.54 \times 10^7$  S/m.

- At the low-frequency end of the spectrum ( $\leq 100$  Hz), the real parts of the responses for the two cases of soil are very close to each other, although they are both very different from the free-space case as expected from (26). As the frequency increases, the responses corresponding to the two soils deviate more and more from each other as the response for the frequency-dependent case moves progressively closer to the free-space response. This behavior may be anticipated from the chosen frequency-dependence of  $\chi(\omega)$  shown in Fig. 2, as the frequency-dependent susceptibility tends to that of free-space at high frequencies.
- The behavior of the imaginary part is more interesting. Initially (up to about 3 kHz in this particular case), the response in the frequency-dependent soil is lower than that in frequency-independent soil, but the former exceeds the latter over the rest of the frequency band of interest. More importantly, there is a slight difference in the frequency of peak response, which is at times proposed as a target identifier, between the two cases.

In Fig. 7, the signals induced by the spherical target buried in two types of soil—one with frequency-independent susceptibility and the other with frequency-dependent susceptibility—are shown along with the signals produced by the soils alone. The following observations are made from the figure.

- The soil signals in both cases dominate the target signal. As already seen, the response from the soil with frequency-independent susceptibility is purely imaginary and linearly dependent on frequency; but the soil with frequency-dependent property has both an imaginary and a real component in its response and they are not linearly dependent on frequency.

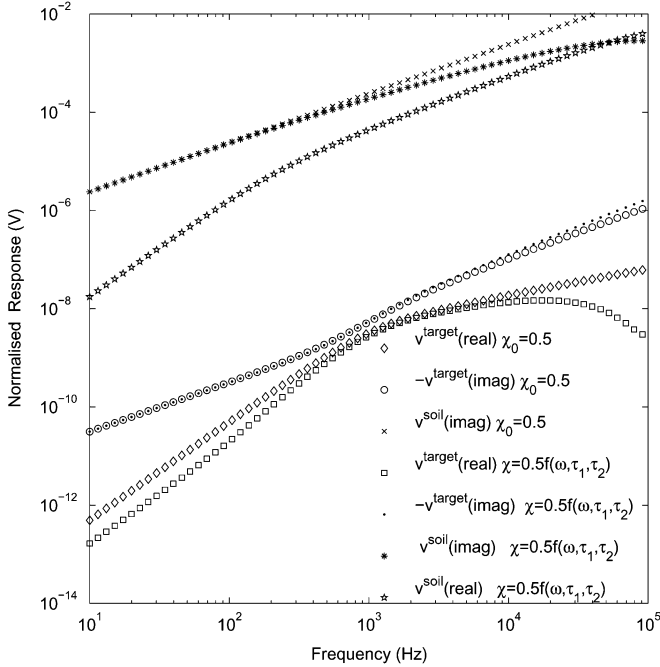


Fig. 7. Comparison of response of a spherical target buried in frequency-independent and frequency-dependent soil. Response of the soil alone is also plotted for comparison. Sensor standoff  $h = 0$  m, object depth  $d = 0.1$  m, soil conductivity  $\sigma_1 = 0$  S/m. The function  $f(\omega, \tau_1, \tau_2)$  represents the term in ( ) in (2).

- The responses of the target buried in the two soils are also different from each other, as is expected from the behavior of the response functions shown in Fig. 6. The real part of the target signal appears to be more affected by the frequency dependence of susceptibility than its imaginary counterpart. It can also be seen that there are frequencies at which the target signal would not be altered by the frequency dependence of susceptibility.

#### D. Target Signal: Conducting Nonmagnetic Soil

As discussed earlier, unlike the case of nonconducting but magnetic soils, an analytical solution for the general case where  $h \neq 0$  and  $a \neq b$  does not appear to be available and hence the soil signal as well as target signal were computed using the numerical technique discussed in [38]. Since only an on-axis target is being considered there is no contribution from the current dipole moment which depends on soil conductivity. The only relevant response functions are those due to the magnetic dipole moment of the target, that is,  $X$  and  $Y$ , which are not dependent on soil conductivity. However, the induced voltage in the receiver coil will be affected by soil conductivity.

In Fig. 8, the induced voltage response of a buried spherical target for two values of soil conductivity (0.01 and 5 S/m) are shown and are compared to the response of the soil alone. A conductivity of 0.01 S/m is considered typical (although values could be much lower) and 5 S/m is likely higher than the conductivity of soil saturated with sea water. The following observations are made from the figure.

- Unlike in the case of frequency-independent soil (shown in Fig. 5) the signal due to the soil has both a real and an imaginary component.

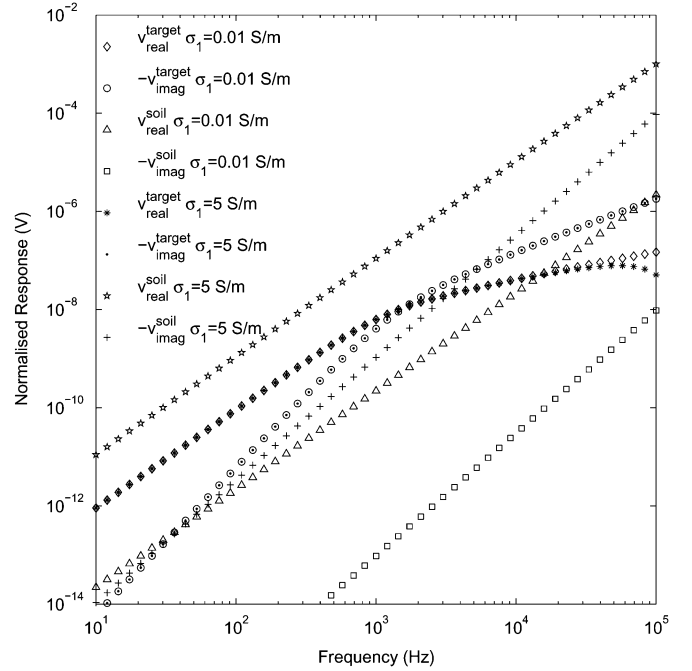


Fig. 8. Response of a buried spherical target for two values of soil conductivity (0.01 and 5 S/m). Response of the soil alone is also plotted for comparison. Sensor standoff  $h = 0$  m, object depth  $d = 0.1$  m, soil susceptibility  $\chi_0 = 0$ .

- The imaginary part of the target response is not noticeably affected by the value of soil conductivity over the frequency band of interest.
- The real part of the target signal is noticeably affected only at the high end of the frequency band.

#### E. Effect of Sensor Standoff

Results presented in Sections III-A, III-C2, and III-D were limited to the case of the sensor head lying on the soil surface ( $h = 0$  m). Of course, the signal due to the soil is expected to decrease as the sensor head is moved away from the ground. In order to get an idea of this variation with sensor height from the ground, the amplitude of the soil signal at a chosen frequency (1000 Hz) is plotted in Fig. 9 for the three types of soil considered. The higher values of  $\chi_0$  and  $\sigma_1$  are chosen to emphasize soil signals. The following observations are made from the figure.

- The signals from magnetic soils are orders of magnitude bigger than that from even the most conductive soil considered.
- The signals from magnetic soils decrease much faster with increasing sensor standoff than do the signal from the conductive soil. Over the 0.5 m standoff range, the signal decreases by more than two orders of magnitude for magnetic soil while it decreases by about an order of magnitude for conductive soil.
- In both cases, there is an initial fast rate of decrease which slows down as the sensor head is elevated.

## IV. SUMMARY AND CONCLUSION

An analytical framework, based on existing work in geophysics and nondestructive testing, for studying the effects of

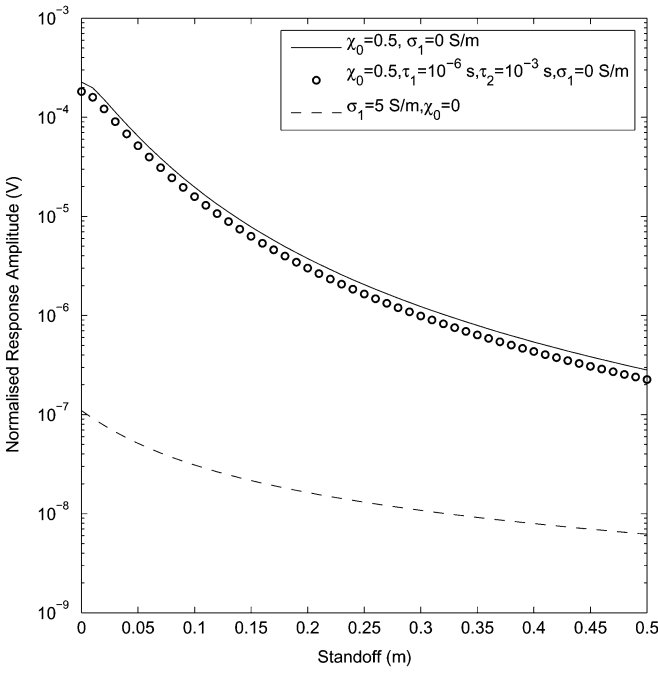


Fig. 9. Variation of amplitude of soil signal at a chosen frequency (1000 Hz) with sensor standoff from the ground.

soil electromagnetic properties on the functioning of metal detectors was outlined. The analysis was applied to three selected simple cases of practical importance, namely, nonconducting soil with frequency-independent susceptibility, nonconducting soil with frequency-dependent susceptibility and nonmagnetic soil with constant conductivity.

Using suitable approximations, a number of simple analytical results were derived to clarify the nature of the response produced by the three soil types. These results were also used to explain a number of previous experimental and field observations by others. Results showed that, in practice, soil magnetic susceptibility would have a far greater influence on metal detector performance than its electrical conductivity. As well, a soil with frequency-independent susceptibility and one with frequency-dependent susceptibility will affect frequency-domain and time-domain detectors differently.

Spectral response of a small aluminum spherical target buried in the three selected types of soil was computed to provide data, albeit very limited, to simulate the possible effect of soil on the signal produced by a small metal part in a landmine. Computations indicated that, in some cases, which could represent practical landmine detection scenarios, the signal from the soil can dominate that due to the target, making it hard to detect the target. Further, a magnetic soil can affect not only the resultant induced signal in a detector but also the response functions often assumed to “uniquely” represent a target. This observation implies that, contrary to present practice, object identification techniques should take into account the electromagnetic parameters of the host medium.

Future work should include further analysis and computation involving a wide range of realistic targets and soil parameters. Such work should also consider the fact that metal pieces in “plastic” landmines have complicated shapes and geometry and are not in contact with the host soil. However, the most pressing

deficiency is the serious lack of measured data both on relevant soil properties and on the response of targets buried in soil, which are needed to verify analysis and computation.

## APPENDIX I FIELDS IN SOIL

Because measurements are only made with sensors in the air, fields in the soil are not commonly considered. Moreover, the response of a buried object is often approximated by adding the response of the soil half-space to the response of the object in air. A better approximation of the response of a buried object should result if fields in the soil are taken into account in the analysis. For easy reference the expressions for the fields are included here. Using results from [11] the fields at a point  $(\rho_0, \phi_0, -d)$  in the soil having parameters  $\sigma_1$  and  $\chi' + i\chi''$  can be written, neglecting displacement currents and using definitions and normalizations similar to those in [39]<sup>6</sup> as

$$H_{1\rho} = -\frac{\pi a^2 I}{2\pi d^3} \int_0^\infty \frac{J_1(A\xi)}{(A\xi/2)} \times \frac{\xi^2(\beta^2 + iH'^2)^{1/2}}{\xi(1 + \chi') + i\xi\chi'' + (\beta^2 + iH'^2)^{1/2}} \times \exp(-Z\xi) \exp[-(\beta^2 + iH'^2)^{1/2}] J_1(D\xi) d\xi \quad (28)$$

$$H_{1z} = \frac{\pi a^2 I}{2\pi d^3} \int_0^\infty \frac{J_1(A\xi)}{(A\xi/2)} \times \frac{\xi^3}{\xi(1 + \chi') + i\xi\chi'' + (\beta^2 + iH'^2)^{1/2}} \times \exp(-Z\xi) \exp[-(\beta^2 + iH'^2)^{1/2}] J_0(D\xi) d\xi \quad (29)$$

$$E_{1\phi} = -\frac{\pi a^2 I}{2\pi d^3} \mu_0 \omega d [-\chi'' + i(1 + \chi')] \times \int_0^\infty \frac{J_1(A\xi)}{(A\xi/2)} \times \frac{\xi^2}{\xi(1 + \chi') + i\xi\chi'' + (\beta^2 + iH'^2)^{1/2}} \times \exp(-Z\xi) \exp[-(\beta^2 + iH'^2)^{1/2}] J_1(D\xi) d\xi \quad (30)$$

where

$$\xi = \lambda d \quad A = a/d \quad Z = h/d, \quad D = \rho_0/d \\ H'^2 = \sigma_1 \mu_0 \omega (1 + \chi') d^2 \quad \beta^2 = \xi^2 - \sigma_1 \mu_0 \omega \chi'' d^2. \quad (31)$$

Putting  $\chi' = 0$  and  $\chi'' = 0$  in (28) and (29), one gets the results given in [39] for the corresponding fields. This should provide a partial check on the validity of these expressions.

## ACKNOWLEDGMENT

The author would like to thank G. West and R. Bailey (University of Toronto), J. E. McFee (DRDC Suffield), and G. Cross (Terrascan Geophysics) for the fruitful discussions we have had on the subject matter presented in this paper.

## REFERENCES

- [1] L. S. Russell, “Detection of land mines (part I),” *Can. Army J.*, vol. 1, no. 5, Nov. 1947.
- [2] ———, “Detection of land mines (part II and III),” *Can. Army J.*, vol. 1, no. 6, Dec./Jan. 1947/48.

<sup>6</sup>Computational results presented in [39, Figs. 4(a) and 5(b)] appear to be erroneous.

- [3] R. J. Roberts, E. Sampson, M. Striker, and T. E. Stewart, "Performance of the SCR-625 Mine Detector over different rocks and soils," U.S. Army Eng. Res. Devel. Labs., Fort Belvoir, VA, Tech. Rep., Jul. 1949.
- [4] J. C. Cook and S. L. Carts, Jr., "Magnetic effects and typical properties of topsoils," *J. Geophys. Res.*, vol. 67, no. 2, pp. 815–828, Feb. 1962.
- [5] B. H. Candy, "Pulse induction time domain metal detector," U.S. Patent 5 576 624, Nov. 1996.
- [6] Y. Das *et al.*, Ed., "Final report of the International Pilot Project on Technology Co-Operation (IPPTC) for the evaluation of metal/mine detectors," European Commission, Joint Research Center, Ispra, Italy, Tech. Rep. EUR 19719 EN, Jun. 2001.
- [7] L. R. Pasion, S. D. Billings, and D. Oldenburg, "Evaluating the effects of magnetic soils on TEM measurements for UXO detection," presented at the *UXO/Countermine Forum*, Orlando, FL, Sep. 2002.
- [8] S. D. Billings, L. R. Pasion, D. W. Oldenburg, and J. Foley, "The influence of magnetic viscosity on electromagnetic sensors," in *Proc. Int. Conf. Requirements and Technologies for the Detection, Removal and Neutralization of Landmines and UXO*, vol. 1, H. Sahli, A. M. Bottoms, and J. Cornelis, Eds., Brussels, Belgium, Sep. 2003, pp. 123–130.
- [9] F. Borry, D. Güle, and A. Lewis, "Soil characterization for evaluation of metal detector performance," in *Proc. Int. Conf. Requirements and Technologies for the Detection, Removal and Neutralization of Landmines and UXO*, vol. 1, H. Sahli, A. M. Bottoms, and J. Cornelis, Eds., Brussels, Belgium, Sep. 2003, pp. 115–122.
- [10] C. Bruschini, "A multidisciplinary analysis of frequency domain metal detectors for humanitarian demining," Ph.D. dissertation, Vrije Univ., Brussels, Belgium, 2002.
- [11] Y. Das, "A preliminary investigation of the effects of soil electromagnetic properties on metal detectors," *Proc. SPIE*, vol. 5415, pp. 677–690, Apr. 2004.
- [12] ———, "Electromagnetic induction response of a target buried in conductive and magnetic soil," *Proc. SPIE*, vol. 5794, pp. 263–274, Mar. 2005.
- [13] G. Cross, "Soil properties and GPR detection of landmines—A basis for forecasting and evaluation of GPR performance," Def. Res. Establish. Suffield, Medicine Hat, AB, Canada, Contract Rep. DRES CR 2000-091, Oct. 1999.
- [14] W. L. Gans, R. G. Geyer, and W. K. Klemperer, "Suggested methods and standards for testing and verification of electromagnetic buried object detectors," Nat. Inst. Standards Technol., U.S. Dept. Commerce, Gaithersburg, MD, NISTIR 89-3915R, Mar. 1990. DTIC AD-A226 626.
- [15] R. Thompson and F. Oldfield, *Environmental Magnetism*. London, U.K.: Allen and Unwin, 1986.
- [16] C. E. Mullins, "Magnetic susceptibility of the soil and its significance in soil science—A review," *J. Soil Sci.*, vol. 28, pp. 223–246, 1977.
- [17] G. R. Olhoeft, "Time dependent magnetization and magnetic loss tangents," M.S. thesis, Mass. Inst. Technol., Cambridge, May 1972.
- [18] C. E. Mullins and M. S. Tite, "Magnetic viscosity, quadrature susceptibility, and frequency dependence of susceptibility in single-domain assemblies of magnetite and maghemite," *J. Geophys. Res.*, vol. 78, no. 5, pp. 804–809, Feb. 1973.
- [19] C. E. Mullins, "The magnetic properties of the soil and their application to archaeological prospecting," *Arch.-Phys.*, vol. 5, pp. 143–347, 1974.
- [20] M. Dabas, A. Jolivet, and A. Tabbagh, "Magnetic susceptibility and viscosity of soils in a weak time varying field," *Geophys. J. Int.*, vol. 108, pp. 101–109, 1992.
- [21] M. Dabas and J. R. Skinner, "Time-domain magnetization of soils (VRM), experimental relationship to quadrature susceptibility," *Geophysics*, vol. 58, no. 3, pp. 326–333, Mar. 1993.
- [22] S. Chikazumi, *Physics of Magnetism*. New York: Wiley, 1964.
- [23] T. Lee, "The effect of a superparamagnetic layer on the transient electromagnetic response of a ground," *Geophys. Prospect.*, vol. 32, pp. 480–496, 1984.
- [24] G. Richter, "Über die magnetische nachwirkung an carbonyleisen," *Ann. Physik*, vol. 29, 1937.
- [25] G. F. West and R. C. Bailey, "An instrument for measuring complex magnetic susceptibility of soils," *Proc. SPIE*, vol. 5794, pp. 124–134, Mar. 2005.
- [26] M. L. Burrows, "A theory of eddy current flaw detection," Ph.D. dissertation, Univ. Michigan, Ann Arbor, 1964.
- [27] Y. Das and J. E. McFee, "A simple analysis of the electromagnetic response of buried conducting objects," *IEEE Trans. Geosci. Remote Sens.*, vol. 29, no. 2, pp. 342–344, Mar. 1991.
- [28] T. Lee, "Transient electromagnetic response of a sphere in a layered medium," *Pure Appl. Geophys.*, vol. 119, pp. 309–338, 1981.
- [29] ———, "The transient electromagnetic response of a conducting sphere in an imperfectly conducting half-space," *Geophys. Prospect.*, vol. 31, pp. 766–781, 1983.
- [30] F. S. Grant and G. F. West, *Interpretation Theory in Applied Geophysics*. New York: McGraw-Hill, 1965.
- [31] I. J. Won, D. A. Keiswetter, and T. H. Bell, "Electromagnetic induction spectroscopy for clearing landmines," *IEEE Trans. Geosci. Remote Sens.*, vol. 29, no. 4, pp. 703–709, Apr. 2001.
- [32] D. Güle. (2000, Dec.) International Detector Test. [Online]. Available: <http://www.itep.ws/pdf/>
- [33] Y. L. Luke, *Integrals of Bessel Functions*. New York: McGraw-Hill, 1962.
- [34] T. Lee, "Transient electromagnetic response of a magnetic or superparamagnetic ground," *Geophys.*, vol. 49, no. 7, pp. 854–860, Jul. 1984.
- [35] M. J. Aitken and C. Colani, "Utilization of magnetic viscosity effects in soils for archaeological prospection," *Nature*, vol. 212, pp. 1446–1447, Dec. 1966.
- [36] M. N. Nabighian, Ed., *Electromagnetic Methods in Applied Geophysics*. ser. Investigations in Geophysics no. 3. Tulsa, OK: Soc. Explor. Geophys., 1987, vol. 1 and 2.
- [37] T. Lee and R. Lewis, "Transient EM response of a large loop on a layered ground," *Geophys. Prospect.*, vol. 22, pp. 430–444, 1974.
- [38] W. L. Anderson, "Computer program numerical integration of related Hankel transforms of orders 0 and 1 by adaptive digital filtering," *Geophysics*, vol. 44, no. 7, pp. 1287–1305, Jul. 1979.
- [39] J. R. Wait and K. P. Spies, "Subsurface electromagnetic fields of a circular loop of current located above ground," *IEEE Trans. Antennas Propagat.*, vol. AP-20, no. 4, pp. 520–522, Jul. 1972.



**Yogadhis Das** (S'75–M'77–SM'88–F'00) received the B.S. degree in electronics and electrical communication engineering from the Indian Institute of Technology, Kharagpur, the M.S. degree in electrical engineering from the University of New Brunswick, Saint John, NB, Canada, and the Ph.D. degree in electrical engineering from the University of Manitoba, Winnipeg, MB, Canada, in 1970, 1972, and 1977, respectively.

He has been with the Threat Detection Group, Defence R&D Canada—Suffield, Medicine Hat, AB, since 1977, where most of his work has been in electromagnetic methods of location and identification of hidden explosive objects. His current research interest is in understanding the effect of soil on landmine detection devices.